DEPLETING IMMUNOSUPPRESSIVE CELLS WITH TUMOR CELLS TO OVERCOME ACQUIRED RESISTANCE TO PD-1 BLOCKADE

BY

ZIYU WANG

A Thesis Submitted to the Graduate Faculty of

WAKE FOREST UNIVERSITY GRADUATE SCHOOL OF ARTS AND SCIENCES

in Partial Fulfillment of the Requirements

for the Degree of

MASTER OF SCIENCE

Biomedical Science

May 2022

Winston-Salem, North Carolina

Approved By:

Yong Lu, Ph.D., Advisor

Guangxu Jin, Ph.D., Chairperson

Mikhail (Misha) Nikiforov, Ph.D.

ACKNOWLEDGEMENTS

Foremost, I would like to give my sincere gratitude to Dr. Yong Lu, my lab PI and mentor for my two-year graduate study in immunotherapies. Thank you for providing me with an awesome and comfortable research lab setting and helping me with no hesitation. Thank you for bringing me into this scientific discovery world and expanding my expertise.

I would like to give my special thanks to Dr. Gang Xue for guiding me in my graduate research studies, and I highly appreciate his help with the design of this work. In addition, my completion of this research could never be accomplished without the additional help of Dr. Ningbo Zheng, Dr. Kun Han, Dr. Muhammad Kalim, and Jing Fang. They always provided supportive suggestions for my experimental difficulties and assisted with some lab techniques I was not familiar with.

I offer my special thanks to my family for my educational and financial support during my studying abroad periods. Thank you for always giving me strong backing to let me chase my dreams.

Finally, I would like to give my thanks to my committee members, Dr. Yong Lu, Dr. Guangxu Jin, and Dr. Mikhail Nikiforov, for their willingness to discuss and critique my master's research study.

Contents

LIST OF ILLUSTRATIONS

LIST OF ABBREVIATIONS

ADC: Antibody-drug Conjugate

APC: Antigen-presenting Cell

αCD73-Dye: IR-700 dye-conjugated anti-Cluster of Differentiation 73 monoclonal antibody

αPD-1: Programmed cell Death-1 monoclonal antibody

CD4: Cluster of Differentiation 4

CD8: Cluster of Differentiation 8

CD45: Cluster of Differentiation 45

CD73: Cluster of Differentiation 73

CTL: Cytolytic T Lymphocytes

CTLA-4: Cytotoxic T-lymphocyte Associated Protein 4

DC: Dendritic Cell

DMSO: Dimethyl Sulfoxide

EDTA: Ethylenediaminetetraacetic Acid

FACS: Fluorescence-activated Cell Sorting

FBS: Fetal Bovine Serum

GITR: Glucocorticoid-Induced TNFR-Related

HPD: Hyperprogression

ICB: Immune Checkpoint Blockade

ICI: Immune Checkpoint Inhibitor

IFNγ: Interferon-gamma

LAG-3: Lymphocyte-activation Gene 3

mAb: Monoclonal Antibody

MDSC: Myeloid-derived Suppressor Cell

MoMDSC: Monocytic Myeloid-derived Suppressor Cell

NIR-PIT: Near-infrared Photoimmunotherapy

PBS: Phosphate Buffered Saline

PD-1: Programmed cell Death 1

PI: Propidium Iodine

PMN.MDSC: Neutrophils and Polymorphonucler Myeloid-derived Suppressor Cell

SCC: Squamous Cell Carcinoma

TAM: Tumor-Associated Macrophage

Th1: T-helper 1 cell

TIM-3: T-cell Immunoglobulin Mucin-3

TIGIT: T cell Immunoreceptor with Ig and ITIM domains

TME: Tumor Microenvironment

TNBC: Triple-Negative Breast Cancer

T_{reg}: Regulatory T cell

ABSTRACT

Antitumor therapies exploiting immune checkpoint blockade (ICB) have been showing promising effects in treating cancer in many clinical cases. However, there are malignant tumor variants that appear resistant to those ICB therapies, and those tumor cells that respond to primary ICB therapies often, gradually, become resistant to them.

Our lab discovered a combinational therapy approach that utilized a common antigen marker, CD73, shared by both tumor cells and major types of immunosuppressive cells in the tumor microenvironment (TME), to effectively eradicate advanced tumor. It is critical that depleting all major types of immunosuppressive cells drastically inhibit immune regulations and suppressions which are supportive for tumor burden.

In addition, combinational targeting with PD-1 ICB further augmented the overall efficacies of the therapies. Administrating IR700-CD73-antibody-dye conjugates and PD-1 monoclonal antibody with near-infrared (NIR) irradiation to the grown solid tumor sites can successfully eradicate tumor to avoid later refractory response.

Our study demonstrated that the depleting of both tumor cells and surrounding immunosuppressive cells effectively eradicate tumor by overcoming the acquired resistance of the tumor cells to ICB.

Introduction

1.1. Immunotherapy and PD-1 Immune Checkpoint Blockade

Along with the increasing diversity in cancers, many different therapies have been developed to be applied in clinic to treat cancer patients. Immunotherapies, derived from utilizing human bodies' own immune system to attack tumor cells, have been showing premise and tremendous effects in treating cancers by augmenting anti-tumor immunity[1]. To treat cancers, immunotherapy is emerging as a novel modality. After a long time of applying traditional target therapy and chemotherapy, improved understanding of malignant tumor evasion to the immune system and novel development of utilizing immune-modulating agents have exploited highly potential opportunities to treat cancer[2,3]. It has been recently demonstrated that immune checkpoint blockade (ICB) is remarkably effective in re-activating tumor-specific T cells across a wide range of tumor types[4]. One of the most typical ICBs is called PD-1 ICB therapy. Targeting PD-1 was a well-developed and successful cancer immunotherapy that illustrated the importance of immune checkpoint signaling in regulating antitumor responses[5]. PD-1 protein molecule, on T cells, binds to PD-L1 or PD-L2 on tumor cells to block positive antitumor signaling via T-cell receptors and CD28 co-stimulatory molecule[6]. The application of PD-1 utilizing anti-PD-1 and anti-PD-L1 recently brought unprecedented efficacies in treating various cancers in the clinic, and therefore, PD-1 ICB stood out as one of the most popular and enlightening approaches in immunotherapies[7] .

1.2. Primary resistance

Primary resistance is defined as the situations that patients do not respond at all to immune checkpoint inhibitors (ICIs) or other immunotherapies and instead progress quickly or eventually[8]. It is highly possible that there exist tumor variants that do not exhibit typical tumor characteristics which make them not responsive to corresponding cancer therapies. In some cases, the extremely limited numbers of systemic T cells could also minimize the efficacy of PD-1 ICB[9]. In clinic, immunotherapies do not work with high efficiency when a malignant tumor has primary resistance, or intrinsic resistance[10].

1.2.1. Primary resistance incidence rate

It has been reported that the majority of patients do not respond to ICB therapies, and that only a very small percentage of patients achieve long-lasting improvement[11]. The incidence rate of primary resistance was about 60-90% in many cancer types, resulting in low responses to cancer therapies[12]. For instance, unfortunately, programmed cell death protein 1 (PD-1) ICB therapy only had an overall response rate of 4.7% in 170 patients with metastatic triple-negative breast cancer (TNBC) in clinic[11] , and PD-L1 blockade even had a worse response rate than the former[12]. In clinical trials using anti-PD1 and anti-PD-L1 treatment for patients with pancreatic ductal adenocarcinoma (PDAC), no response has been observed (0%) so far [11,13]. Accordingly, it can be explained that the effects of ICB are negated by immune tolerance mechanisms, which keep the immune system under control[14]. Immune tolerance regulates immune pro-inflammatory pathways and interferes with anti-tumor signaling, and it is one of the most critical factors that dampen subsequent therapies in later advanced tumor stages[15].

1.2.2. Mechanism of primary resistance

It is emerging that tumor-associated macrophages (TAMs), myeloid-derived suppressor cell (MDSCs), and regulatory T cells (T_{reg} cells) function to suppress the induction, infiltration, and cytolytic function of $CD8^+$ CTLs and promote immune tolerance[16]. It is important to highlight that when tumors are nonresponsive or resistant to ICB treatment, such immunosuppressive phenotypes are not eliminated by ICB[17–22]. Especially in clinical cases, ICB therapies have been showing extremely limiting efficacy in treating relapsed and resistant tumors.

1.2.2.1. Regulatory T cell (T_{reg} cell)

T_{reg} cell population consists of mainly $CD4^+$ T cells which suppress the anti-tumor immune response to promote tumor progression[19]. Various cancer types exhibiting increased intratumoral T_{reg} numbers have been associated with a poor prognosis, including breast, melanoma, pancreatic, colorectal, ovarian, and lung cancers[18]. Activated T_{reg} cells in TME can inhibit the activation of effector $CD4^+$ T cells and cytotoxic $CD8^+$ T cells and furtherly restrict the consumption of IL-2 and proliferation of them[17].

1.2.2.2. Tumor-associated macrophage (TAM)

TAMs are key players that support the immunosuppressive mechanisms in TME, and they are the most abundant cell type that can be detected in most solid tumors[23,24]. They have one of the 2 activating phenotypes of macrophages called M2, and this M2 phenotype

triggers the expression of immune inhibitory molecule PD-L1 and the release of IL-10 which is classified as anti-inflammatory cytokines[25,26].

1.2.2.3. Myeloid-derived suppressor cell (MDSC)

MDSCs are myeloid precursor cells halted at variable stages of differentiation, which are found within the TME, where they are responsible for immunosuppressive effects. In clinical situations, the number of MDSCs in TME has been confirmed to have a positive correlation with poor disease prognosis[27]. In addition, MDSCs have also been responsible for the signaling pathways that lower the $CD8^+$ T cell: T_{reg} cell ratio in intratumoral environment[28] and promote the synthesis of immunosuppressive mediators including prostaglandin E2 (PGE2) and enzymes, such as arginase-1 (ARG1) and inducible nitric oxide synthase (iNOS)[29]. These immunosuppressive mediators play significant roles in inhibiting T cells cell cycle, their migration to tumor sites, and their cytotoxic functions in antigen-specific tumor killing[22,30].

1.3. Acquired resistance

With expanded use of ICB immunotherapies and a higher level of activity, the number of patients who show a tumor response has increased, as well as the chances of finding patients who responded for a period of time and then progressed, termed acquired resistance[8]. Acquired resistance against cancer therapies is common, and identifying the causative factors and discovering underneath mechanisms are significant to break through

the barriers of resistance and recurrence[31,32]. Targeting tumor-specific antigens could select the resistant variant tumors and make them outgrow in TME. When ICB is administrated, an acquired resistance would be somewhat inevitable[33,34].

1.3.1. Acquired resistance incidence rate

The prevalence of acquired resistance across various tumor types is not clearly characterized in routine reports as opposed to primary resistance[35]. However, there are estimated rates of acquired resistance collected by previous studies based on the available duration of response data among different tumor types. For example, the acquired resistance incidence rate of head and neck squamous cell carcinoma (SCC) after 1 line therapy of pembrolizumab is 54%, and the rate is 60% for melanoma after 1 line therapy of ipilimumab**.** Among certain types of tested tumors, melanoma is one example showing there is a negative correlation between the acquired resistance rate and the overall response rate[20,21]. However, in the vast majority of tumor types, there is no remarkable correlation between those two variables, so investigating the underneath mechanisms of acquired resistance becomes a more challenging exercise[8].

1.3.2. Potential mechanism of acquired resistance

For the mechanism of acquired resistance, there is very limited understanding about it. Nonetheless, there are proposed and inferred mechanisms that were constructed based on the established principles of cancer therapies**.** These speculated mechanisms can be roughly classified into several categories: (1) neoantigen depletion; (2) tumor-mediated immunosuppression/exclusion; (3) defects in antigen presentation; (4) IFN-y signaling;

and (5) additional inhibitory checkpoints[36]. Above all, immunosuppressive cells might play a significant role in acquired resistance, based on the previous study showing evidence that ICB therapy itself had very limited impact on depleting immunosuppressive cells, and some surrounding immune cells in TME could inhibit the functioning of ICB[37,38].

1.4. Potential approach to overcome acquired resistance

1.4.1. Current approach to target single type of immunosuppressive cells

Currently there are some well-established approaches to target single type of immunosuppressive cells. For instance, to target M2-like TAMs, CSF1 was clinically applied in recent clinical trials[39]. As for T_{reg} cells, CD25 was a potential therapeutic target that was clinically tested[40]. All-trans retinoic acid (ATRA) was utilized as an ICI to target MDSCs and reduce their immunosuppressive genes, such as PD-L1, IL-10, and indoleamine 2,3-dioxygenase[41]. Nonetheless, recent clinical studies of the relevant techniques have shown that if only one or a few types of those immunosuppressive cells are targeted, others will have high potentials to compensate and interfere with anti-tumor immunity[42,43]. Moreover, there is no developed approach to target single type of immunosuppressive cells without affecting their counterpart effector cells. As a result, the existed targeting efforts to ablate immunosuppressive cells did not produce the expected curative results in cancer treatment.

1.4.2. Targeting one type of immunosuppressive cells may affect its counterpart effector cell

Since immunosuppressive cells, many are myeloid-derived, consist of a heterogenous population, it is necessary to develop therapies specifically targeting MDSCs, TAMs, and DCs, while minimizing adverse effects on other myeloid cells (DCs), in order to overcome ICB resistance. Furthermore, nearby T_{reg} cells may also suppress the function of tumor infiltrating CTLs [44]. A successful immune therapy also depends on controlling tumor infiltrating T_{reg} cells[45]. Since both Th1 cells and CTLs have most of the T_{reg} cell markers[44], there must be an approach to specifically deplete tumor infiltrating T_{reg} cells without damaging wanted CTLs in anti-tumor responses.

1.4.3. Immunosuppressive cells may also be associated with acquired resistance

Although immune cells in the TME decreases responsiveness to ICB therapies and may play a part in acquired resistance to ICB immunotherapy, it remains unclear what role they play in this process[46]. Because ICB would not inhibit those immunosuppressive cells, we hypothesized that those immunosuppressive cells are also associated with acquired resistance based on the previous findings and clinical records about immunosuppressive cells playing significant roles in primary resistance of many cancer types.

1.4.4. Develop an approach to reduce major types of immunosuppressive cells

Aside from a few published studies evaluating the characteristics or mechanisms of acquired resistance to ICIs, there have been no approved therapeutic breakthroughs for circumventing acquired resistance as of date[34]. Due to the high possibility of systemic depletion of immunosuppressive cells leading to severe autoimmune disease[47], comprehensive ablation of all kinds of immunosuppressive cells in tumors (from MDSCs to TAMs and Tregs) may lead to tremendous immunotherapeutic efficacy, fulfilling an unmet need where tumor immune landscapes need to be modified to overcome resistance mechanisms. To date, there are no approaches that target a particular type of immunosuppressive cell in the TME. We wanted to discover an approach that can simultaneously reduce those 3 major types of immunosuppressive cells without affecting CTLs and other immune effector and cytolytic cells.

Results

2.1. Relapse of resistant tumors occurs when only targeting a tumor-expressed antigen.

2.1.1. Objectives

To demonstrate that relapse of resistant tumor is inevitable when only applying PD-1 ICB therapy or targeting tumor-specific antigen, we wanted to recapitulate the fact of acquired resistance or resistance after treatments by using a mouse model, and we also aimed to achieve the goal of specific tumor-killing of $EMT6^{B7H3}$ cells, a commonly used murine breast tumor cell line with tumor antigen B7H3 overexpression.

2.1.2. Methods

2.1.2.1. Mice

For the mice, we used female BALB/c strains to conduct in vivo experiments, and they were purchased from the Jackson Laboratory. The female mice were not used to conduct experiments until they reached 6 to 8 weeks old. All the experiments complied with the protocols approved by the Institutional Animal Care and Use Committee and Institutional Review Board at the Wake Forest University School of Medicine.

2.1.2.2. Cell lines

For the cell line we used, the EMT6 cell line was purchased from ATCC. Cells were cultured in RPMI 1640 medium (Invitrogen) supplemented with 10% heat-inactivated fetal bovine serum (FBS, Thermo Fisher Scientific), 100 U/ml penicillin-streptomycin, and 2 mM L-glutamine (both from Invitrogen).

2.1.2.3. Reagents

ViaStain AO/PI staining solution (catalogue no. CS2-0106) was purchased from Nexcelom. Propidium iodide (PI) solution (catalogue no. 421301) was purchased from BioLegend. CellTrace CFSE Cell Proliferation Kit (catalogue no. C34554) was purchased from Thermo Fisher. LIVE/DEAD Fixable Blue Dead Cell Stain Kit (catalogue no. L23105) was purchased from Thermo Fisher. Anti-mouse CD73 antibody (clone: TY/23, catalogue no. BE0209), anti-mouse B7H3 antibody (clone: MJ18, catalogue no. BE0124), anti-mouse PD-1 antibody (clone: RMP1-14, catalogue no. BE0146), anti-mouse CTLA-4 antibody (clone: UC10-4F10-11, catalogue no. BE0032), anti-mouse GITR antibody (clone: DTA-1, catalogue no. BE0063), anti-mouse TIGIT antibody (clone: 1G9, catalogue no. BE0274), anti-mouse LAG-3 antibody (clone: C9B7W, catalogue no. BE0174), anti-mouse TIM-3 antibody (clone: RMT3- 23, catalogue no. BE0115), anti-mouse OX-40 antibody (clone: OX-86, catalogue no. BE0031), anti-mouse 4-1BB antibody (clone: LOB12.3, catalogue no. BE0169), anti-mouse NK1.1 antibody (clone: PK136, catalogue no. BE0036), anti-mouse CD4 antibody (clone: GK1.5, catalogue no. BE0003-1) and anti-mouse CD8 antibody (clone: 2.43, catalogue no. BE0061) were purchased from BioXcell.

2.1.2.4. Flow cytometry

Tumors were dissected, manually dissociated, and enzymatically digested in PBS containing 2% FBS for 20 minutes at room temperature with Collagenase D (Sigma) and DNase I (Roche). EDTA was added to a final concentration of 10 mM, and the suspension was incubated for an additional 5 minutes at room temperature. To obtain a single-cell suspension, the entire suspension was filtered using a 70 m cell strainer. After Fc blocking, FITC-, PE-, APC-, or eFluor-conjugated mAbs (1:100 dilution) were utilized for staining. For sorting, samples were collected using a Fortessa flow cytometer, and data was processed using Flowjo software. The $CD45^+$ immune cells were identified by consensus clustering of the antibodies for cell lineage markers: DCs ($CD11c^{hi}MHCII^{hi}CD24^+$), M1-like TAM (TAM.M1, $CD11b^{hi}F4/80^+MHCII^{int/hi}CD206^-CD24^-$), TAM.M2 ($CD11b^-F4/80^+MHCII^{low/neg}CD206^+CD24^-$), Mo-MDSC ($CD11b^{hi}Ly6C^{hi}Ly6G^{low}$), PMN-MDSC ($CD11b^{hi}Ly6G^h$), B cells ($CD19^+$), $CD8^+$ T cells ($CD3^+CD8^+$), T_{reg} cells ($CD3^+CD4^+Foxp3^+$), $CD4^+$ effector ($CD3^+CD4^+Foxp3^-$) and NK cells ($Nkp46^+$).

2.1.2.5. Construction of IR700-dye conjugated antibodies

The construction of IR-700-dye conjugated antibodies are shown (Fig. 1). IR700-Dye conjugated antibodies were prepared using IRDye 700DX Protein Labelling Kits (catalogue no. 928-38046, Licor). In short, antibodies were incubated with IRDye 700DX NHS Ester at room temperature in phosphate buffer (pH 8.0) for 1 hour. The product of the biochemical conjugation process was then purified using Zeba Spin Desalting Column. The antibody concentrations were determined by BCA Protein Assay Kit (catalogue no. 23225, Thermo Fisher), and the concentration of IR700DX NHS Ester was determined by measuring the absorption at 689 nm. The number of IR700 molecules conjugated to each

antibody was calculated as reported by our previous study[48] and others[49]. Antibody conjugates used in this study contained an average of 3.5 molecules of IR700 on each antibody.

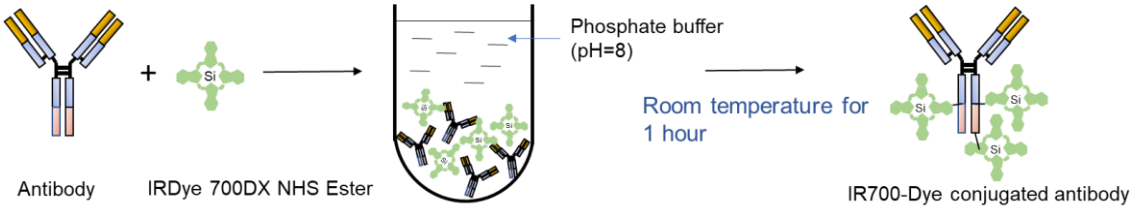

Figure 1| Schematic overview of construction of IR700-dye conjugated antibodies.

2.1.2.6. Live/dead cell assay

Cancer cells or sorted immune cells (1×10^4) were plated into 96-well plates and incubated with IgG, IgG-Dye, αB7H3-Dye, or αCD73-Dye at 5 μg/mL for 6 hours at 37 °C with 5% CO_2. The cells were then washed with cold PBS two times and cultured with phenol red-free cell culture medium. Cells were then irradiated by a NIR light-emitting diode at wavelengths of 690 nm (catalogue no. L690-66-60, Marubeni America). To measure the cytotoxic effect of NIR, cells were stained with PI 2 hours after irradiation, and then approximate 5,000 cells/events were collected and analyzed by flow cytometry. In some experiments, treated cells were incubated with Nexcelom ViaStain AO/PI staining solution (catalogue no. CS2-0106) in the dark for 20 minutes at room temperature, and the representative images were captured on a Nikon TE300 fluorescence microscope.

2.1.2.7. Mice in vivo tumor model

BALB/c mice were inoculated at the left mammary gland with 5×10^5 EMT6 tumor cells with or without i.v. injection of 1×10^5 EMT6 tumor cells, respectively. Treatments were started on day 5 or 7 when tumor size reached about 130 mm^3.

Mice were randomized into different groups and mAb-Dye (100 μg) was i.v. injected 1 d before NIR treatment. The tumors in mammary glands were exposed once or twice to 690 nm NIR with a total dose of 100 J/cm^2 for each NIR irradiation. In some experiments, 150 μg αPD-1 was intraperitoneally (i.p.) injected every 3 days starting on day 5 or 7 for a total of 4 injections in EMT6 tumor-bearing mice or 5 injections for mice with spontaneous TNBC tumors. All other parts of mice were covered with aluminum film to avoid light exposure. Mice were monitored daily after treatment. The tumor was measured using a caliper and tumor size was calculated as $0.5 \times length \times width^2$. Mice were euthanized using carbon dioxide and subsequent cervical dislocation.

2.1.2.8. qPCR

Total RNA was extracted from the tumor using the TRIzol Reagent (Thermo Fisher), followed by complementary DNA synthesis with the High-Capacity cDNA Reverse Transcription kit (Applied Biosystems). qPCR was conducted with SYBR Select Master Mix (Applied Biosystems). Expression was normalized to the expression of the housekeeping gene β-actin. mB7H3 forward: 5′-ATGCTTCGAGGATGGGGTG-3′, mB7H3 reverse: 5’ - CCAGGCTCTGGGGAAAAGG - 3; mβ-actin forward: 5’ - GGCTGTATTCCCCTCCATCG - 3’, mβ - actin reverse: 5’ - CCAGTTGGTAACAATGCCATGT - 3’.

2.1.2.9. Statistical analysis

For statistical analysis, Student's t-test, or analysis of variance (ANOVA) was used. Survival was analyzed using the log-rank test. A P value less than 0.05 was considered statistically significant. Results are presented as mean ± s.d. unless otherwise indicated.

2.1.3. Results

To initially observe the occurrence of acquired resistance in ICB, we utilized EMT6^{B7H3} cells-bearing mice (overexpression of B7H3 on EMT6 TNBC cells; figure 2).

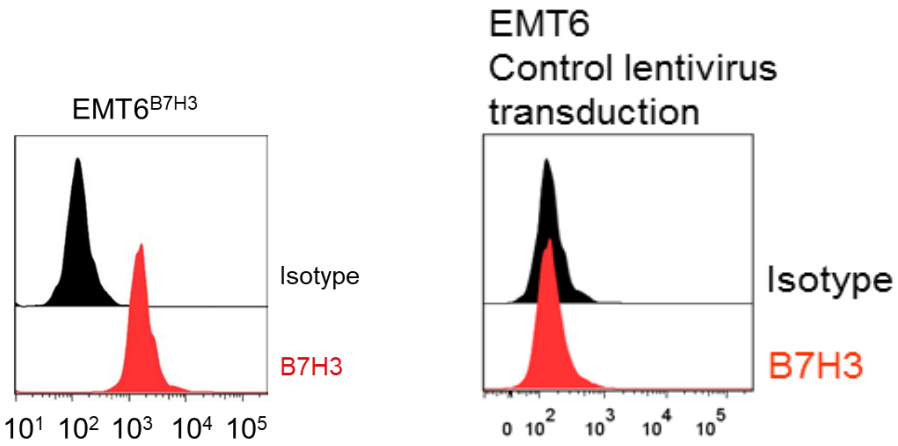

Figure 2| The surface expression of B7H3 on EMT6^{B7H3} cancer cells was assessed by FACS.

In order to achieve tumor-killing of EMT6^{B7H3} cells, we utilized an existing photo-depletion technique based on NIR using antibody-IR700 conjugates[50–52]. αB7H3-Dye + NIR induced drastic cell necrosis in >95% of EMT6^{B7H3} tumor cells *in vitro*, and the results were measured (Fig. 3).

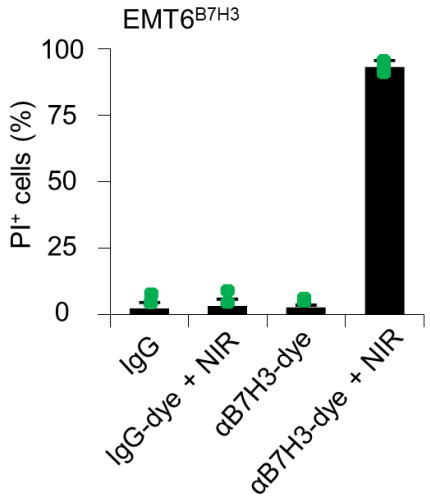

Figure 3| EMT6^{B7H3} cells were treated as indicated in vitro. The percentage of dead cells was determined by FACS after PI staining (n= 3 biological replicates).

Then, we inoculated EMT6^{B7H3} cells via mammary glands and tail veins of mice. After EMT6^{B7H3} cells were inoculated in mice, αPD-1, αB7H3-Dye + αPD-1, and αB7H3-Dye + NIR treatments all induced a partial response initially the tumor-bearing mice, but unfortunately, the progression of acquired resistance eventually led to tumor relapse *in vivo* (Fig. 4). Although the combinational treatment with ICB αB7H3-Dye+NIR+αPD-1 could further inhibit the growth of EMT6^{B7H3} tumors (with longer inhibiting strength) compared with αPD-1, αB7H3-Dye + αPD-1 or αB7H3-Dye + NIR treatments, all respondent tumors still finally relapsed (Fig. 4). The recurred progress was similar to the scenario of relapse and acquired resistance in the clinical case, with a median survival time of 46.5 d for αB7H3-Dye + NIR and 48.5 d for αB7H3-Dye + NIR + αPD-1 treated mice (Fig. 4).

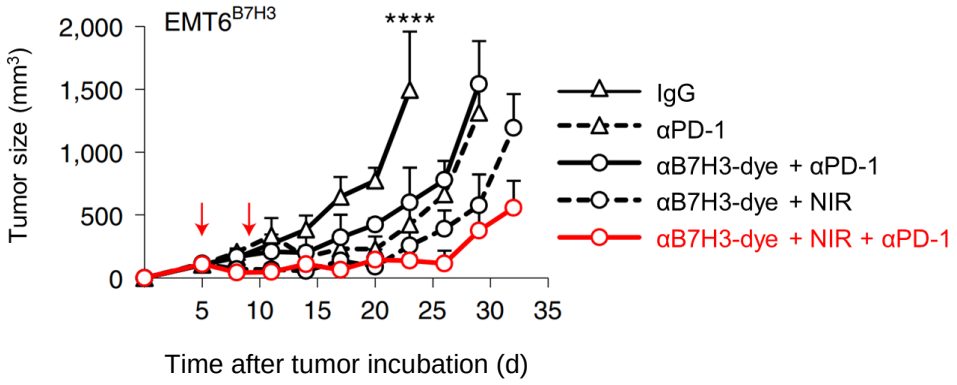

Figure 4| Orthotopic tumor growth curves. BALB/c mice bearing both orthotopic EMT6^{B7H3} tumor (5×10^5 EMT6^{B7H3} tumor cells injected in the mammary gland) and lung metastasis tumors (1×10^5 EMT6^{B7H3} tumor cells injected via tail vein) were treated on day 5 with control IgG, αPD-1, αB7H3-Dye + αPD-1, αB7H3-Dye + NIR or αB7H3-Dye + NIR + αPD-1 (combo). NIR irradiation was given on the orthotopic tumor only (other parts of the mice were shielded from light). n= 5 mice per group. Red arrows represent NIR irradiation. ****P< 0.0001, IgG group compared with αPD-1, αB7H3-Dye + αPD-1, αB7H3-Dye + NIR or combo group, two-way ANOVA with Holm–Sidak test for multiple

We next inoculated two EMT6^{B7H3} tumors of mice and performed the αB7H3-Dye + NIR + αPD-1 treatment (the tumors were either untreated or treated with αB7H3-Dye + NIR+ αPD-1 combo therapy). We therefore hypothesized that recurrent tumors would be B7H3-loss variant tumors iteratively selected by αB7H3-Dye + NIR targeting B7H3, as often occurs in clinical cancer targeted therapy. To test our hypothesis, we collected PBS-treated EMT6^{B7H3} tumor, EMT6 tumor, locally recurrent EMT6^{B7H3} tumor and remote EMT6^{B7H3} tumor tissues on day 23. Quantitative PCR (qPCR) demonstrated that only treated and relapsed EMT6^{B7H3} tumors showed largely downgraded *B7H3* levels (Fig. 5).

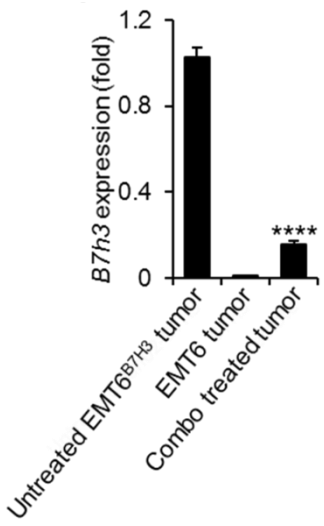

Figure 5| qPCR analysis of *B7h3* gene levels of EMT6^{B7H3} tumor tissues harvested on day 23 as shown in Figures 4. EMT6^{B7H3} and EMT6 tumors are also used as controls (n=3 biological replicates). IgG-Dye represents IR-700 dye-conjugated IgG, *α*B7H3-Dye represents IR-700 dye-conjugated anti-B7H3 mAbs. Representative results from one of two repeated experiments are shown. Data are mean ± SD. ****P<0.0001, Combo treated group compared with Untreated EMT6^{B7H3} tumor group, one-way ANOVA with Tukey's correction.

2.1.4. Conclusion

Taken together, these results demonstrate that specifically targeting variant tumor cells, and obviously, the formation of resistant variant tumor cells is inevitable even though PD-1 ICB was co-administrated. However, to fully achieve our goal in overcoming acquired resistance, we still need to test our suggested approach in further experiments.

2.2. Identification of common marker(s) to target some major types of immunosuppressive cells.

2.2.1. Objectives

Since tumors contain a great amount of infiltrated immunosuppressive cells that may restrain the functioning of immunotherapy[53], we hypothesized that additional targeting, except to tumor themselves, of immunosuppressive cells in the TME would surmount the acquired resistance to ICB. To achieve the goal of removing those immunosuppressive cells, we needed to find and identify a common marker that is highly expressed by those cells.

2.2.2. Methods

2.2.2.1. Rank-adjusted fold-change analysis

Based on their gene expression comparisons between 'non-immunosuppressive and immunosuppressive cells', the genes were categorized according to their degree of gene expression change. We defined the rank ri by sorting the overall fold-change of gene i, ni , from high to low:

$$n_i = \sum_{j=1}^{3} S_{ij}$$

where $S_{ij} = \begin{cases} 0 \text{ if } FC_{ij} < 5 \\ 1 \quad \text{else} \end{cases}$, FC_{ij} is the gene expression fold-change of gene *i* compared with *j*. The rank-adjusted fold-change integrated from the three comparisons is defined as follows

$$FC_{ij} = \frac{\sum_{j=1}^{3} S_{ij} F_{ij}}{3}$$

2.2.2.2. Live/dead cell assay

Cancer cells or sorted immune cells (1×10^4) were plated into 96-well plates and incubated with IgG, IgG-Dye, αB7H3-Dye, or αCD73-Dye at 5 μg ml−1 for 6 hours at 37 °C with 5% CO_2. The cells were then washed with cold PBS twice and cultured with phenol red-free culture medium. Cells were then irradiated with a NIR light-emitting diode at wavelengths of 690 nm (catalogue no. L690-66-60, Marubeni America). To measure the cytotoxic effect of NIR, cells were stained with PI 2 h after irradiation, and then ~5,000 cells/events were analyzed by flow cytometry. In some experiments, treated cells were incubated with Nexcelom ViaStain AO/PI staining solution (catalogue no. CS2-0106) at room temperature in the dark for 20 minutes, and then representative images were captured on a Nikon TE300 fluorescence microscope.

2.2.2.3. Venn diagram analysis based on cut-tree algorithm

To compare the gene expression profiles of Treg cells, MDSCs and TAM.M2 cells to Th1 cells, DCs and normal tissue macrophages, we applied unsupervised hierarchical clustering to all genes (>2-fold increase) in the published microarray data. The upregulated genes (>2-fold increase) in Treg cells, MDSCs and TAM.M2 cells were taken for commonality analysis by Venn graph. Venn diagram analysis was implemented using Venn Diagram in R (https://www.r-project.org/) as described previously[54].

2.2.2.4. Flow cytometry

Tumors were dissected, manually dissociated, and enzymatically digested in PBS containing 2% FBS for 20 minutes at room temperature with Collagenase D (Sigma) and DNase I (Roche). EDTA was added to a final concentration of 10 mM, and the suspension was incubated for an additional 5 minutes at room temperature. To obtain a single-cell suspension, the entire suspension was filtered using a 70 m cell strainer. After Fc blocking, FITC-, PE-, APC-, or eFluor-conjugated mAbs (1:100 dilution) were utilized for staining. For sorting, samples were collected using a Fortessa flow cytometer, and data was processed using Flowjo software. The $CD45^+$ immune cells were identified by consensus clustering of the antibodies for cell lineage markers: DCs ($CD11c^{hi}MHCII^{hi}CD24^+$), M1-like TAM (TAM.M1, $CD11b^{hi}F4/80^+MHCII^{int/hi}CD206^-CD24^-$), TAM.M2 ($CD11b^-F4/80^+MHCII^{low/neg}CD206^+CD24^-$), Mo-MDSC ($CD11b^{hi}Ly6C^{hi}Ly6G^{low}$), PMN-MDSC ($CD11b^{hi}Ly6G^h$), B cells ($CD19^+$), $CD8^+$ T cells ($CD3^+CD8^+$), T_{reg} cells ($CD3^+CD4^+Foxp3^+$), $CD4^+$ effector ($CD3^+CD4^+Foxp3^-$) and NK cells ($Nkp46^+$).

2.2.2.5. Statistical analysis

For statistical analysis, Student's t-test, or analysis of variance (ANOVA) was used. Survival was analyzed using the log-rank test. A P value less than 0.05 was considered statistically significant. Results are presented as mean ± s.d. unless otherwise indicated.

2.2.3. Results

On the basis of published microarray data, we were able to identify a common marker highly expressed on major types of immunosuppressive cells, to specifically target them. Such a marker is highly expressed on T_{reg} cells, MDSCs, and M2-like TAMs, compared to Th1 cells, DCs, and normal tissue macrophages, respectively[55,56]. According to the clustering analysis, Treg cells, MDSCs, and TAM.M2 cells display very different gene signatures than Th1 cells, DCs, and tissue macrophages, respectively (Fig. 6).

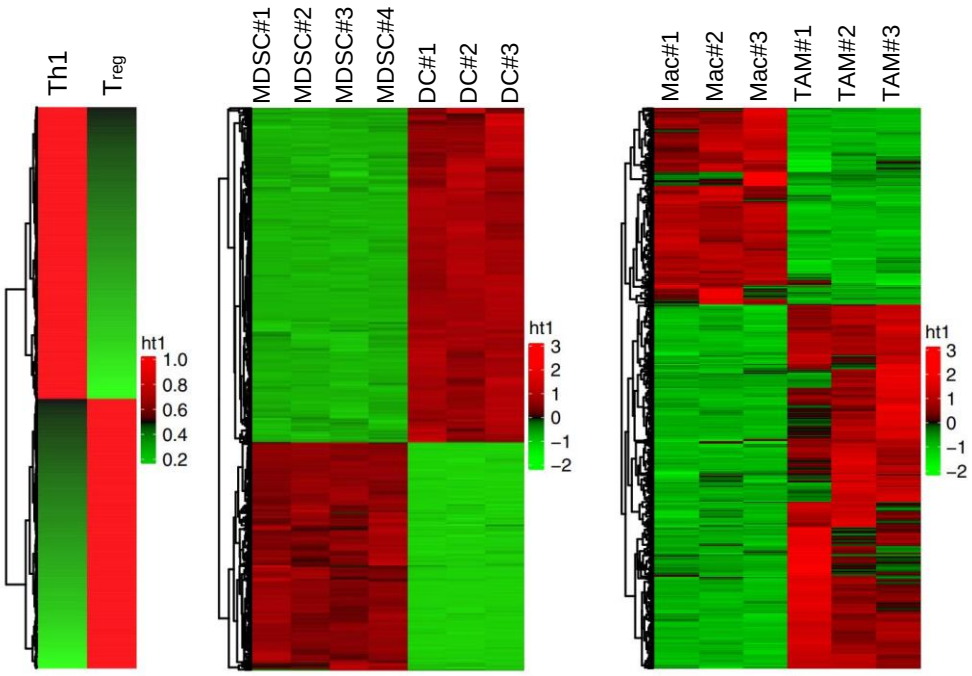

Figure 6| Hierarchical clustering of gene expression of Treg cells and Th1 cells, MDSCs, DCs, TAM.M2 cells, and tissue macrophages. ht1, heatmap.

Further analysis was conducted by using a Venn diagram to determine whether there are overlapping genes (>2-fold upregulation) between TAM.M2/tissue macrophages and Treg

cells/Th1. In contrast to non-immunosuppressive cells, we discovered eleven genes co-expressed in these immunosuppressive cells (Fig. 7).

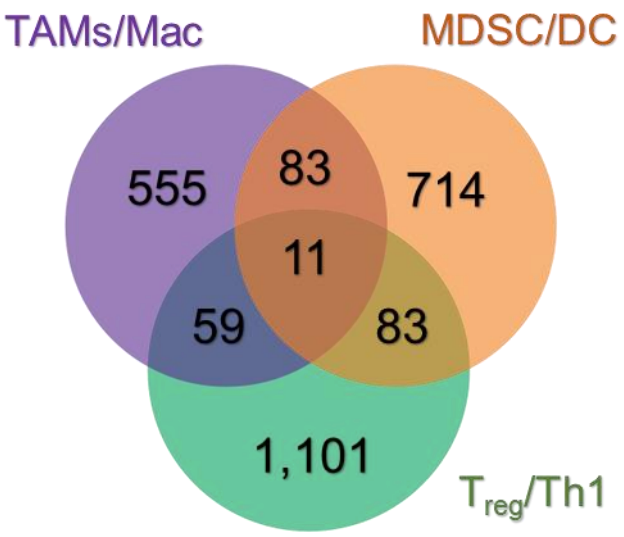

Figure 7| Venn diagrams displaying the number of upregulated genes of T_{reg} cells, MDSCs and TAM.M2 cells.

To rank the genes, fold-changes of their expression levels were incorporated into the comparisons of immune suppressed and non-immune suppressed cells, and the change in each gene's level of expression was calculated utilizing rank-adjusted fold-change (see Methods for details). According to the results, *Nt5e* gene (encodes CD73 protein) ranked highest among 10 other genes (Fig. 8); the result is also in agreement with some previous studies[57,58].

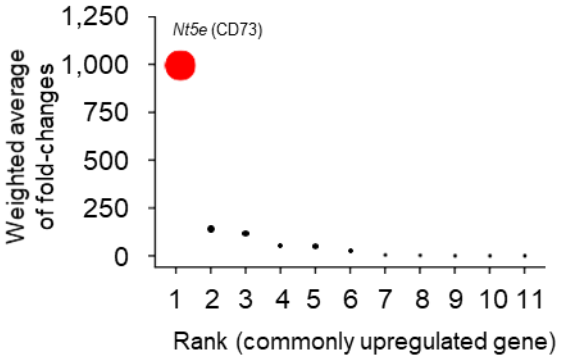

Figure 8| Rank-adjusted fold-change analysis for 11 commonly upregulated genes among Treg cells, MDSCs and TAM.M2 cells.

In a further analysis, we used fluorescence-activated cell sorting (FACS) to identify the types of immune cells present in the EMT6 TME and found that surface CD73 expression was high in several types of immunosuppressive cells (for example, Treg cells, MDSCs and TAM.M2 cells; Figure 9a, b, while such expression was negative or very low for DCs or effector immune cells (for example, effector $CD4^+$ T cells, $CD8^+$ T cells or NK cells) (Fig 10).

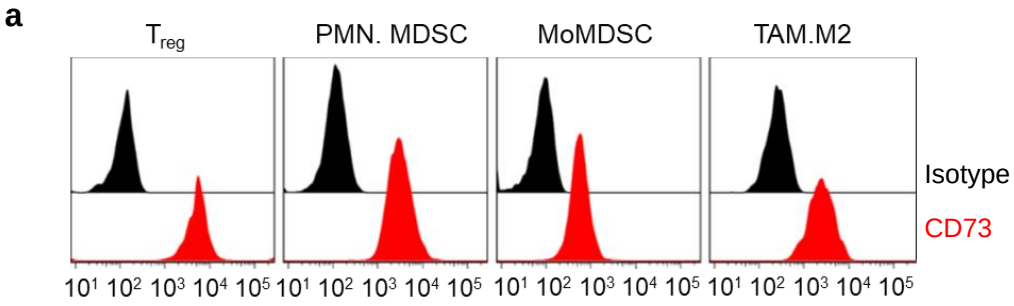

b

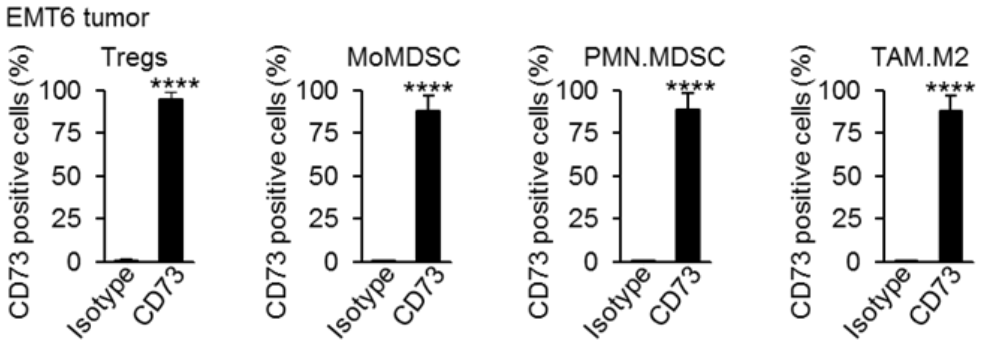

Figure 9| a, Surface expression levels of CD73 on Treg cells, PMN.MDSC, MoMDSC and TAM.M2 cells isolated from EMT6 tumors. **b,** the percentage of $CD73^+$ Tregs, MoMDSC, PMN.MDSC, and TAM.M2 cells isolated from EMT6 tumors were determined by FACS (n=3 biological replicates). Data are mean ± SD. ****P<0.0001, CD73 group compared with Isotype group, unpaired two-tailed Student's t-test (**b**).

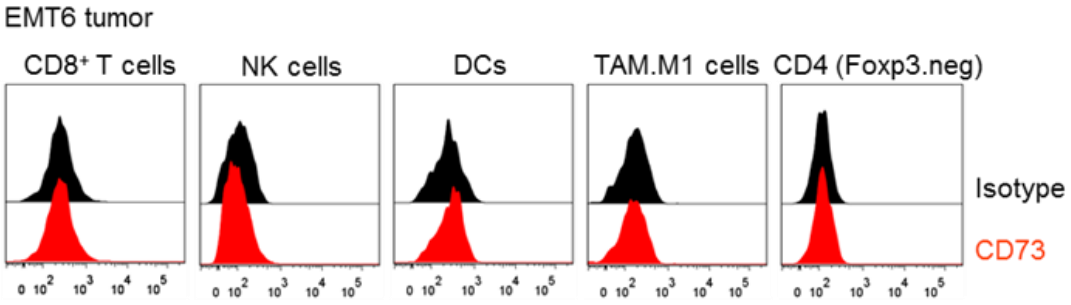

Figure 10| FACS analysis for surface expression of CD73 on $CD8^+$ T cells, NK cells, DCs, TAM.M1 cells, and $CD4^+$ (Foxp3.neg) T cells isolated from EMT6 tumors. Shown are the representative results.

Consequently, CD73 could therefore be used to selectively deplete all major types of immunosuppressive cells in the TME and thus influence the tumor immune landscape. Because we also wanted to deplete the tumor cells along with those immunosuppressive cells at the same time, the expression of the CD73 on tumor cells also need to be checked

and analyzed. There are various types of tumor cells have been reported to express surface CD73[59], we thus analyzed the expression of CD73 using a murine tumor cell line. Interestingly, CD73 was highly expressed on ~75% of murine EMT6 TNBC cells **(Fig. 11)**.

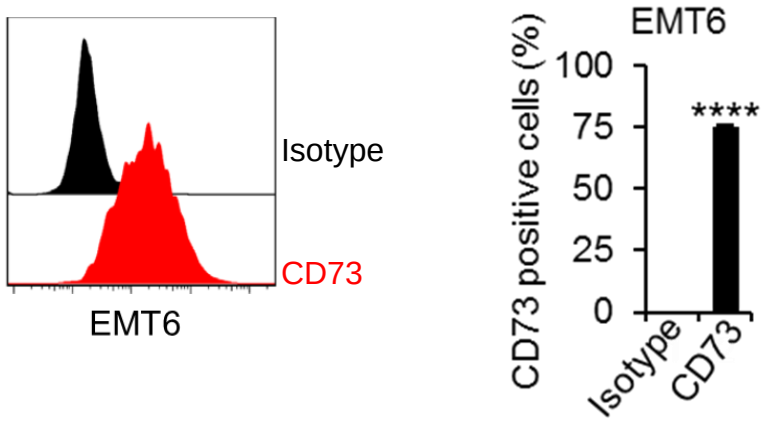

Figure 11| Surface expression levels and percentage of CD73 on EMT6 cancer cells were assessed by FACS. (n=3 biological replicates) Data are mean ± SD. ****P<0.0001, CD73 group compared with Isotype group, unpaired two-tailed Student's t-test.

Using dye-CD73 conjugates, we performed NIR irradiation on CD73+cells to kill local tumor cells and found that αCD73-Dye+NIR induced rapid cell necrosis in ~75% of EMT6 tumor cells **(Fig. 12 and 13)**.

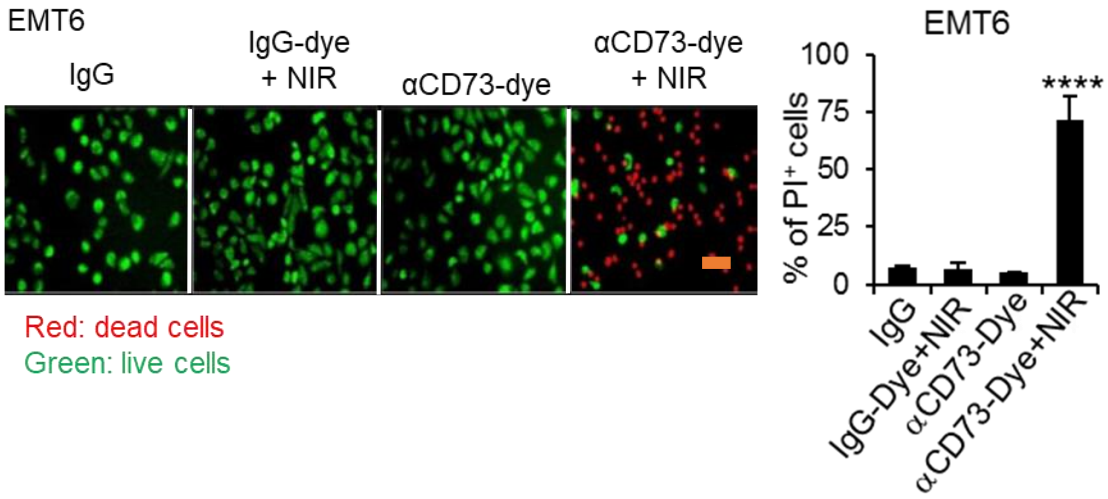

Figure 12| EMT6 cancer cells were treated with IgG, IgG-Dye + NIR, αCD73-Dye or αCD73-Dye + NIR *in vitro* (n=3 biological replicates). Cell death was tested using Nexcelom ViaStain AO/PI staining solution. The percentage of dead cells was determined by FACS after PI staining. Representative images are shown. Data are mean ± SD. ****P<0.0001, αCD73-Dye+NIR group compared with IgG, IgG-Dye + NIR, or αCD73-Dye group, one-way ANOVA with Tukey's correction. Bar scale = 100µm.

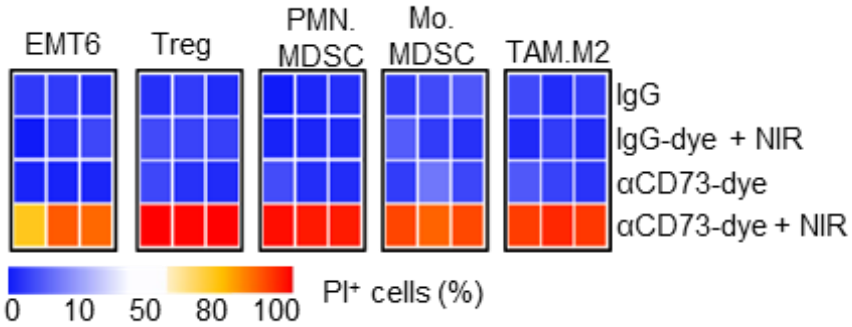

Figure 13| Cell necrosis of tumor cells and Treg cells, PMN.MDSC, MoMDSC and TAM.M2 cells isolated from EMT6 tumors. Cells were treated with IgG, IgG-Dye + NIR, αCD73-Dye or αCD73-Dye + NIR in vitro. Shown is the heatmap illustrating the percentage of PI^+ dead cells tested by FACS (representative results from one of two repeated experiments).

These results serve to support that rapid killing of tumor cells after NIR exposure depends on CD73 expression. The effects of CD73-Dye+NIR on EMT6 tumor-isolated immune cells were then investigated in vitro. CD73-Dye+NIR rapidly destroyed immunosuppressive cells, including Treg cells, MDSCs, and TAM.M2, in association with their surface expression of CD73 **(Fig. 13 and 14)**, while not harming those counterpart CTLs (effector $CD4^+$ T cells and $CD8^+$ T cells), NK cells or DCs **(Fig. 14)**.

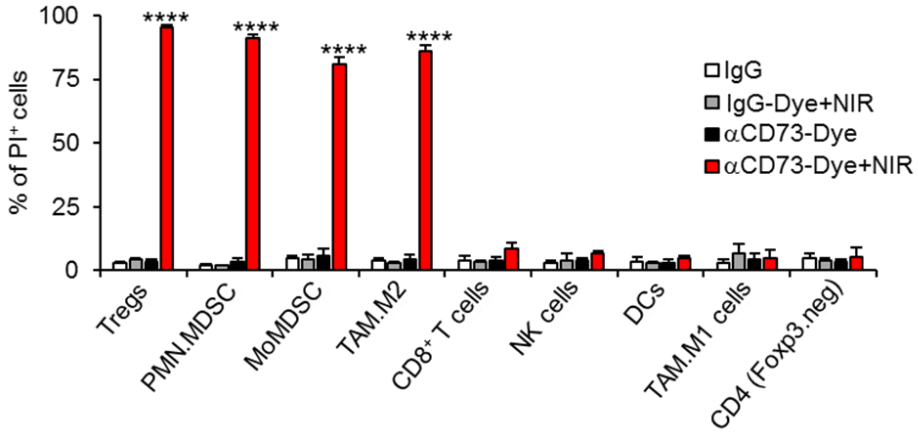

Figure 14| T_{reg}, PMN.MDSC, MoMDSC, TAM.M2, $CD8^+$ T cells, NK cells, DCs, TAM.M1 cells, and $CD4^+$ (Foxp3.neg) T cells were isolated from EMT6 tumors and treated as indicated *ex vivo* (n=3 biological replicates). The percentage of dead cells was determined by FACS after PI staining. IgG-Dye represents IR-700 dye-conjugated IgG, *α*CD73-Dye represents IR-700 dye-conjugated anti-CD73 mAbs. Representative results from one of two repeated experiments are shown. Data are mean ± SD. ****P<0.0001, αCD73-Dye+NIR group compared with IgG, IgG-Dye + NIR, or αCD73-Dye group, one-way ANOVA with Tukey's correction.

These data suggest that CD73-Dye can eliminate tumor cells and the major types of immunosuppressive cell in the TME simultaneously, in a highly specific manner.

2.2.4. Conclusion

These finding serve to support that CD73-Dye can eliminate tumor cells and the major types of immunosuppressive cell, T_{reg} cells, MDSCs, and TAM.M2 cells, in the TME simultaneously, in a highly specific-targeting manner. The found CD73 could be used as the common marker.

2.3. Targeting $CD73^+$ cells alters the immune response in TME and supports CTL responses in vivo.

2.3.1. Objectives

The previous drastic antitumor function on tumors using our suggested approach motivated us to further analyze the EMT6 TME after the treatment of αCD73-Dye-mediated NIR irradiation. We wanted to investigate the tumor TME and observe the underneath immune system responses.

2.3.2. Methods

2.3.2.1. Flow cytometry

Tumors were dissected, manually dissociated, and enzymatically digested with Collagenase D (Sigma) and DNase I (Roche) in PBS containing 2% FBS for 20min at room temperature. EDTA was added to a final concentration of 10 mM and the suspension was incubated at room temperature for an additional 5min. The entire suspension was filtered

through a 70μm cell strainer to obtain a single-cell suspension. FITC-, PE-, APC- or eFluor-conjugated mAbs (1:100 dilution) were used for staining after Fc blocking. Samples were acquired with a Fortessa flow cytometer for sorting, and data were analyzed with Flowjo software.

2.3.2.2. Statistical analysis

For statistical analysis, Student's t-test, or analysis of variance (ANOVA) was used. Survival was analyzed using the log-rank test. A P value less than 0.05 was considered statistically significant. Results are presented as mean ± s.d. unless otherwise indicated.

2.3.3. Results

Here, we used fluorescence activated cell sorting (FACS) to assess tumor immune cell lineages, and the results revealed several intriguing characteristics linked with antitumor immunity activation. αCD73-Dye-mediated NIR irradiation decreased many kinds of immunosuppressive cells in tumors, including an approximate 85% drop in Treg cells, an 80% reduction in TAM.M2, and a 95% reduction in MDSCs. Remarkably, the decrease in immunosuppressive cells was accompanied by a significant rise in tumor-infiltrating $CD8^+$ CTLs, which increased about 50-fold when compared to other treated groups. **(Fig. 15).**

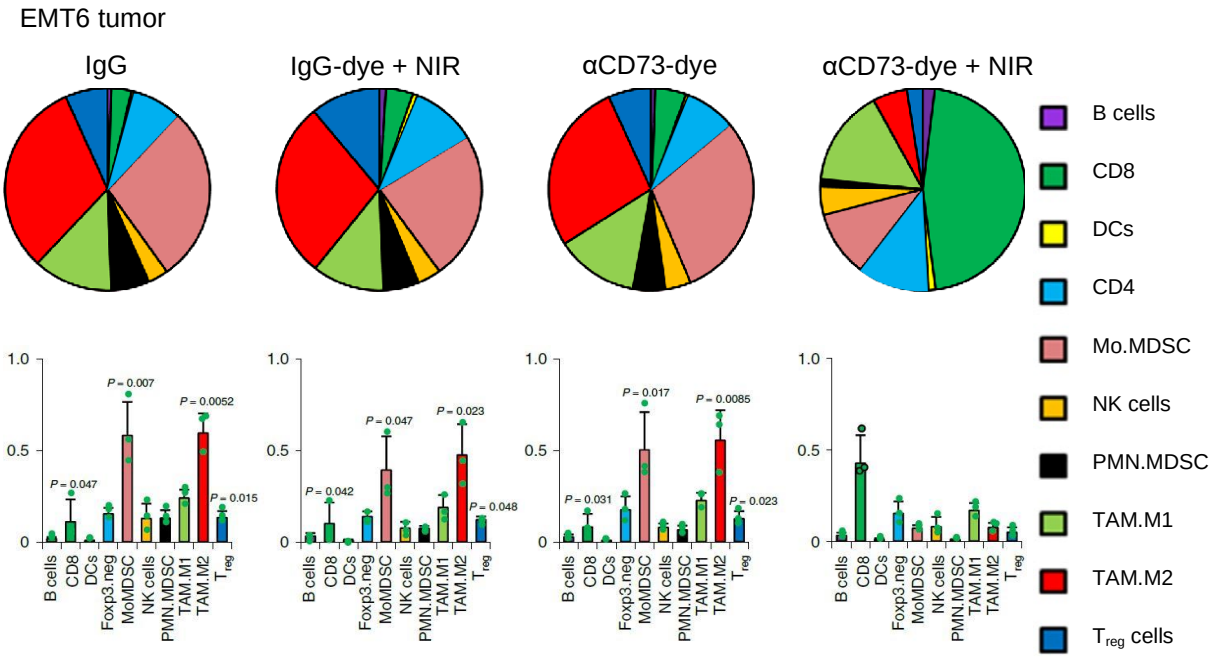

Figure 15| Percentage of EMT6 tumor-infiltrating CD45$^+$ immune cell subsets from the treated tumor-bearing mice. FACS was used to detect cell subsets in tumor tissues. Calculated cell numbers per 100 mg EMT6 tumor are shown by indicated immune cell subset (n= 3 biological replicates). Representative results from one of two repeated experiments are shown. Data are mean ± s.d. ****P< 0.0001, αCD73-Dye + NIR group compared with IgG, IgG-Dye + NIR or αCD73-Dye group, one-way ANOVA with Holm–Sidak test for multiple comparisons.

2.3.4. Conclusion

Overall, these data demonstrates that depletion of CD73$^+$ cells by αCD73-dye + NIR, comparing to IgG, IgG-dye + NIR, or αCD73-dye, in the TME directs and induces significantly greater CD8$^+$ CTLs revitalization for immune elimination of tumor cells.

2.4. αCD73-Dye + NIR + αPD-1 overcomes the acquired resistance to ICB immunotherapy

2.4.1. Objectives

Finally, we wanted to test whether our approach αCD73-Dye + NIR can the acquired resistance of ICB. Since the NIR irradiation has limitations on distal target eradication because it mainly focuses on local site, we wanted to test whether there is an approach that could eradicate both advanced orthotopic and metastatic tumors in our model.

2.4.2. Methods

2.4.2.1. Mice in vivo tumor model

BALB/c mice were inoculated at the left mammary gland with 5×10^5 EMT6 tumor cells with or without i.v. injection of 1×10^5 EMT6 tumor cells, respectively. Treatments were started on day 5 or 7 when tumor size reached about 130 mm^3.

Mice were randomized into different groups and mAb-Dye (100 μg) was i.v. injected 1 day before NIR treatment. The tumors in mammary glands were exposed once or twice to 690 nm NIR with a total dose of 100 J/cm^2 for each NIR. In some experiments, 150 μg αPD-1 was intraperitoneally (i.p.) injected every 3 days starting on day 5 or 7 for a total of 4 injections in EMT6 tumor-bearing mice or 5 injections for mice with spontaneous TNBC tumors. All other parts of mice were covered with aluminum film to avoid light exposure. Mice were monitored daily after treatment. The tumor was measured using a caliper and

tumor size was calculated as 0.5 × length × width 2. Mice were euthanized using carbon dioxide and subsequent cervical dislocation.

2.4.3. Results

This approach was tested on the EMT6 mouse model for antitumor efficacy. For mice bearing advanced orthotopic and lung metastatic EMT6 tumors **(Fig. 16)**, αPD-1, αCD73-Dye +αPD-1 and αCD73-Dye + NIR treatments induced initial tumor regression, with median survival times of 30.5, 30 and 47 days, respectively (22 days for IgG group).

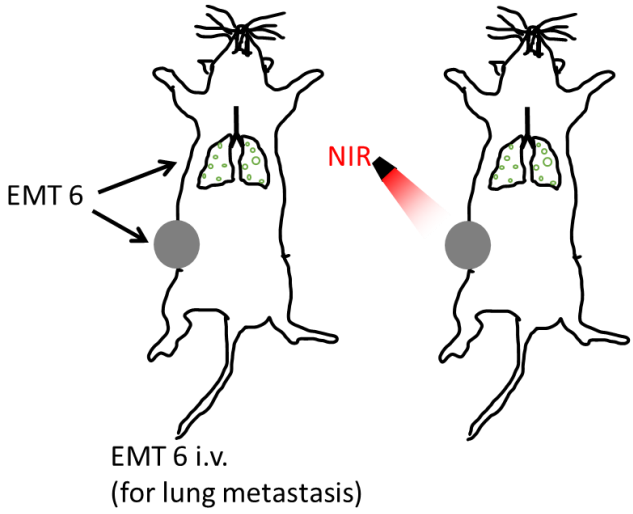

Figure 16| Diagram of the treatments. BALB/c mice bearing both orthotopic EMT6 tumor (5×10^5 EMT6 tumor cells injected in the mammary gland) and lung metastasis tumors (1×10^5 tumor cells injected via tail vein) were treated on day 5 with control IgG, αPD-1, αCD73-Dye +αPD-1, αCD73-Dye + NIR or αCD73-Dye + NIR+αPD-1 (combo). NIR irradiation was given on the orthotopic tumor only (other parts of the mice were shielded from light)

Interestingly, combinational therapy (αCD73-Dye+NIR+αPD-1, hereafter) completely eradicated both advanced orthotopic EMT6 tumor (with NIR) and lung metastatic tumors (no direct NIR to lung) **(Fig. 17, 18)**.

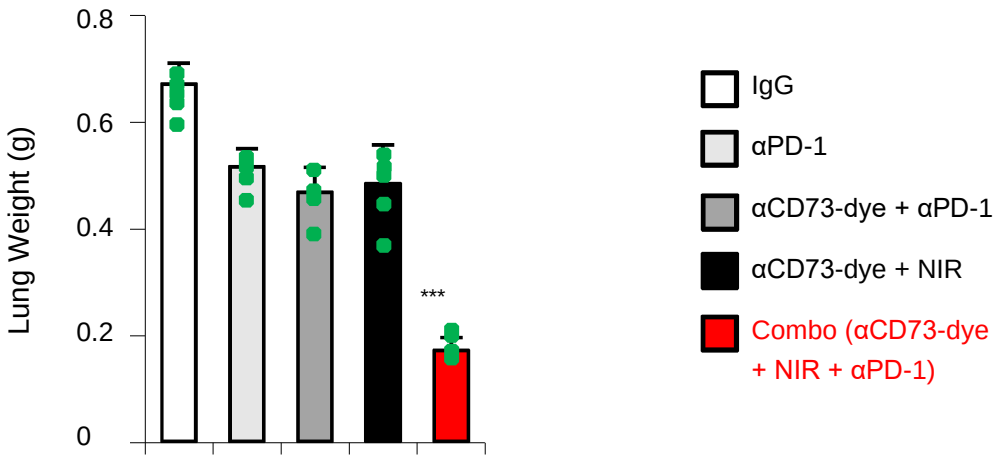

Figure 17| Mice were euthanized on day 20 and the summarized lung weights of mice receiving indicated treatments are shown (n= 5 mice per group). Data are mean ± s.d. ***P< 0.001, combo group compared with IgG, αPD-1, αCD73-Dye +αPD-1 or αCD73-Dye + NIR group, one-way ANOVA with Tukey's correction.

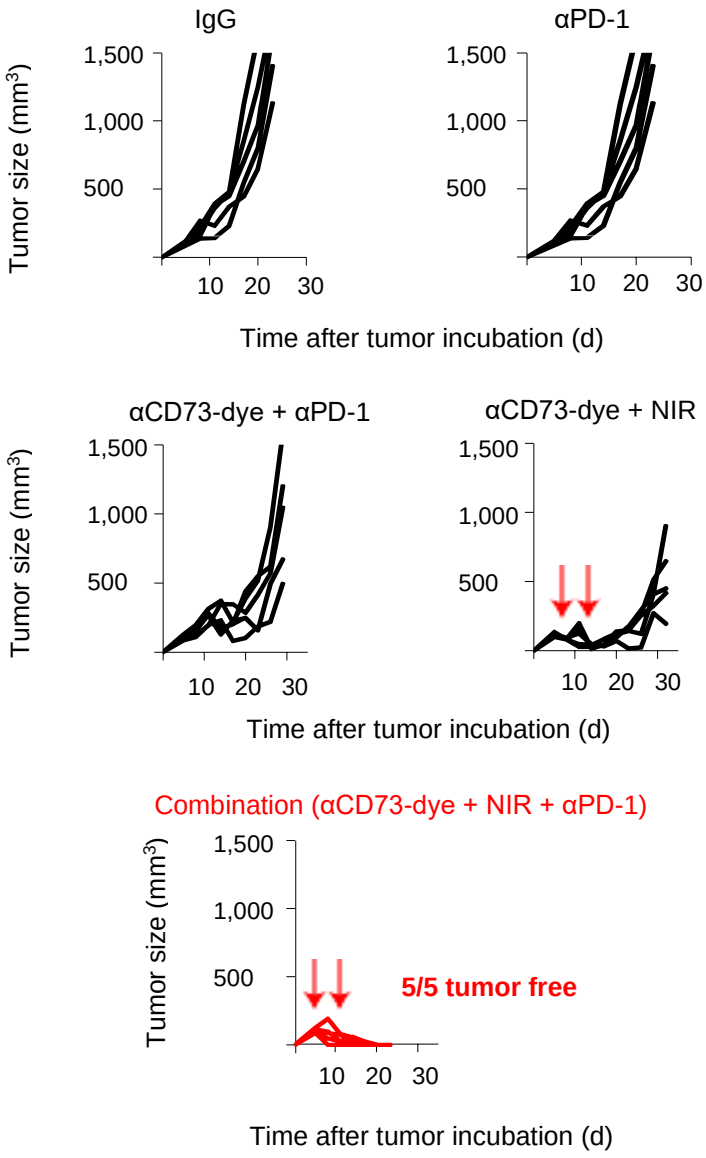

Figure 18| Tumor growth curves (n= 5 mice per group) of the orthotopic EMT6 tumors after indicated treatments. The red arrows represent NIR irradiation.

Additionally, at least 90% of the mice survived 100 days as tumor-free **(Fig. 19)**. The data supports that this combo therapy of αCD73-Dye+NIR+αPD-1 had outstanding efficacy in

tumor killing *in vivo*. The combo therapy could even induce a curative response in those mice.

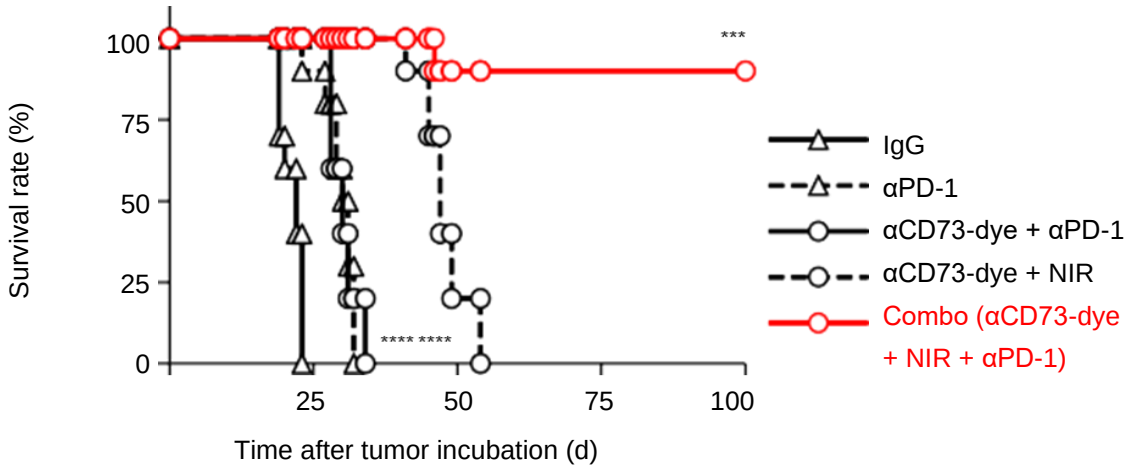

Figure 19| Survival curves of EMT6 tumor-bearing mice (n= 10 mice per group). ***P< 0.001, combo group compared with IgG, αPD-1, αCD73-Dye +αPD-1 or αCD73-Dye + NIR group; ****P< 0.0001, αPD-1 group compared with IgG group; ****P< 0.0001, αCD73-Dye + NIR group compared with IgG, αPD-1 or αCD73-Dye +αPD-1 group, survival analysis was conducted using log-rank test with Holm test for multiple comparisons.

2.4.4. Conclusion

Our results indicated that removing immunosuppressive cells from the local environment might be an effective method to overcome acquired resistance. Consequently, depleting those immunosuppressive cells via the NIR irradiation eradicated advanced tumors, and the combinational therapy of depleting immunosuppressive cells via CD73-dye + NIR irradiation and PD-1 ICB induced further curative and tumor-free responses in mice.

Discussion

In this work, we discovered that acquired resistance can emerge after PD-1 ICB therapies or target therapy combined with PD-1 ICB therapy, and we also discovered a possible role for immunosuppressive cells in the TME that results in tumor recurrence. Our findings also point to an approach for eliminating acquired resistance by deleting all major types of immunosuppressive cells locally. We repurposed anti-CD73 mAbs from blocking the enzymatic activity of CD73 into the killing of $CD73^+$ tumor and immunosuppressive cells by treatment with CD73-Dye + NIR to overcome systemic ICB primary and acquired resistance by identifying CD73 (via bioinformatics analysis) as a common marker highly expressed on various types of immunosuppressive cells. Surprisingly, it was found that in the EMT6 TNBC tumor model conducted, reducing the major types of immunosuppressive cells eliminated advanced tumors, overcame acquired resistance to the PD-1 ICB immunotherapy, and generated curative responses in mice.

Acquired resistance has been associated with many cancer therapy failure and mortality in more than 85% of individuals with advanced malignancies. The heterogeneity of cancer cell populations may result in a response to treatment at first, but recurrence often occurs after treatments. As a result of heterogeneously somatic mutations, the few cancer cells that are resistant to treatment will continually be selected and escape during treatments[33]. When tumor cells die from chemotherapy or targeted therapy, the antigens presented by the tumor become available in extracellular environment, which then facilitates the antitumor response in ICB therapies. It has been demonstrated through our research that targeting tumor cells' expressed antigens (e.g., targeting B7H3 by αB7H3-Dye + NIR +

αPD-1) without destroying the immunosuppressive TME promotes the growth of B7H3-resistant tumor cells, similar to acquired resistance under clinical conditions[60,61].

A number of tumor-infiltrating immune suppressive cells, including T_{reg} cells, MDSCs, and TAM.M2, reduce CTL induction, infiltration, and cytolytic function, diminishing responses to ICB therapy[16,17,19,29,62]. Immunosuppressive cells contribute to acquired resistance in ICB immunotherapy, but their precise mechanisms remain somewhat abstruse. We hypothesized that depleting almost all major types of immunosuppressive cells could make it possible to overcome the acquired resistance in ICB immunotherapy. To date, no approaches have been developed that precisely target a single type of immunosuppressive cell within the TME. By comparing gene profiles of immunosuppressive cells to effector immune cells, we found that CD73 was highly expressed by all major types of immunosuppressive cells. Additionally, we found that immunosuppressive cells, such as MDSCs, Treg cells, and TAMs.M2, highly expressed CD73, whereas $CD8^+$ CTLs, $Foxp3^-$ $CD4^+$ T cells, or DCs had either negative or very low CD73 expression. Based on this unique natural characteristic of those immunosuppressive cells, we would have the opportunity to simultaneously target and remove these immunosuppressive cell subsets, which may contribute to acquired resistance in ICB therapy.

Explicitly, CD73 is the major source of extracellular adenosine, and increased extracellular levels of adenosine may impair the cytotoxic properties of $CD8^+$ T cells and NK cells within the TME[63]. There is a previous research study that showed high expression of CD73 in immunosuppressive cells in tumors, especially in TAM.M2, that contributed to poor clinical outcomes by inhibiting T-cell infiltration. Therefore, anti-CD73 antibodies have been used to target the enzyme activity in CD73 for the treatment of cancer; However, both

pre-clinical studies and clinical trials have shown limited response of advanced tumors to αPD-1 + αCD73 antibody or αPD-1 + adenosine antagonist (clinical effectiveness data don't support launching a phase III study)[64,65]. As a result, in our current investigation, we used CD73-Dye + NIR to target $CD73^+$ cells to induce full response and circumvent recurrence in ICB immunotherapy. This antitumor effect is associated with the rapid killing of $CD73^+$ tumor cells and immunosuppressive cells (including Treg cells, MDSCs, and TAMs.M2 cells), but no or very limited cytotoxicity to effector $CD4^+$ T cells, $CD8^+$ T cells, or DCs, which is correlated with the level of CD73 surface expression.

According to the Human Protein Atlas dataset[66], most cancer tissues have moderate to strong cytoplasmic and membranous CD73 positivity, with lymphomas and testicular malignancies being moderately positive or lacking expression. In addition, normal human skin and breast tissues have relatively low CD73 expression[67]. Although several previous studies have revealed that some cells, such as endothelial cells and hepatocytes[68], express some degree of CD73 and may therefore experience unexpected toxicity when being treated with CD73-Dye + NIR, NIR light irradiation can be performed under endoscopic supervision through a fiber optic diffuser to target specific tumor areas while minimizing potential injury to normal cells. These findings imply that certain tumor types, including breast cancer, may be suitable candidates for local CD73-Dye + NIR irradiation to destroy the tumor and immunosuppressive cells in the TME while causing little harm to normal cells. Furthermore, in patients with PDAC, local photodynamic treatment has been accomplished by utilizing laser fibers injected by needles positioned percutaneously through the anterior abdominal wall and guided by ultrasonography and computed tomography[54]**.** Finally, NIR irradiation with antibody-dye conjugates has been investigated

in phase II clinical trials (NCT02422979; anti-EGFR-IR700), demonstrating that our proposed strategy is potentially practical to be applied in patients.

Nonetheless, there are still many limitations from this research study. First, there is only one type of murine tumor cell line conducted, which highly limits the variety of feasible tumor types of the suggested approach. More types of tumor cell lines, including human tumor cells, need to be conducted for more precise research study. Second, the underneath mechanism of the major immunosuppressive cells contributing to acquired resistance was not well established nor demonstrated. For example, whether single type of those immunosuppressive cells could lead to tumor recurrence and acquired resistance to ICB should be investigated and illustrated to make the research more intact.

By and large, our findings indicate that immunosuppressive cell-mediated acquired resistance occurs in ICB immunotherapy. The findings show that our suggested approach, using αCD73-Dye + NIR + αPD-1, to target tumor cells and immunosuppressive cells in TME selectively and concurrently is adequate for overcoming acquired resistance and triggering a curative response in PD-1 ICB resistant tumor. As a result, this research study may further decorate the groundwork for future clinical trials to treat TNBC and other malignant cancers.

Reference

1. Waldman, A. D., Fritz, J. M. & Lenardo, M. J. A guide to cancer immunotherapy: from T cell basic science to clinical practice. *Nat. Rev. Immunol.* **20**, 651–668 (2020).

2. Esteva, F. J., Hubbard-Lucey, V. M., Tang, J. & Pusztai, L. Immunotherapy and targeted therapy combinations in metastatic breast cancer. *Lancet Oncol.* **20**, e175–e186 (2019).

3. Chouaid, C. *et al.* Cost-effectiveness analysis of pembrolizumab versus standard-of-care chemotherapy for first-line treatment of PD-L1 positive (>50%) metastatic squamous and non-squamous non-small cell lung cancer in France. *Lung Cancer* **127**, 44–52 (2019).

4. Reck, M. *et al.* Pembrolizumab versus Chemotherapy for PD-L1–Positive Non–Small-Cell Lung Cancer. *N. Engl. J. Med.* **375**, 1823–1833 (2016).

5. Qin, W. *et al.* The Diverse Function of PD-1/PD-L Pathway Beyond Cancer. *Front. Immunol.* **10**, 1–16 (2019).

6. Freeman, B. G. J. *et al.* Engagement of the PD-1 Immunoinhibitory Receptor by a Novel B7 Family Member Leads to Negative Regulation of Lymphocyte Activation. **192**, (2000).

7. Lei, Y., Li, X., Huang, Q., Zheng, X. & Liu, M. Progress and Challenges of Predictive Biomarkers for Immune Checkpoint Blockade. **11**, 1–14 (2021).

8. Sharma, P., Hu-lieskovan, S., Wargo, J. A. & Ribas, A. Review Primary , Adaptive , and Acquired Resistance to Cancer Immunotherapy. *Cell* **168**, 707–723 (2017).

9. Zuazo, M. *et al.* Systemic CD4 Immunity as a Key Contributor to PD-L1/PD-1 Blockade Immunotherapy Efficacy. *Front. Immunol.* **11**, 1–10 (2020).

10. Nguyen, A. T., Shiao, S. L. & Mcarthur, H. L. Advances in Combining Radiation and Immunotherapy in Breast Cancer. 143–152 (2021) doi:10.1016/j.clbc.2021.03.007.

11. Shimizu, T., Seto, T., Hirai, F. & Takenoyama, M. Phase 1 study of pembrolizumab (MK-3475 ; anti-PD-1 monoclonal antibody) in Japanese patients with advanced solid tumors. 347–354 (2016) doi:10.1007/s10637-016-0347-6.

12. Vonderheide, R. H. *et al.* Tremelimumab in Combination with Exemestane in

Patients with Advanced Breast Cancer and Treatment-Associated Modulation of Inducible Costimulator Expression on Patient T Cells. 3485–3494 doi:10.1158/1078-0432.CCR-10-0505.

13. Segal, N. H. *et al.* Preliminary data from a multi-arm expansion study of MEDI4736, an anti-PD-L1 antibody. *J. Clin. Oncol.* **32**, 3002 (2014).

14. Granier, C. *et al.* Mechanisms of action and rationale for the use of checkpoint inhibitors in cancer. 1–8 (2017) doi:10.1136/esmoopen-2017-000213.

15. Siegel, R. L. & Miller, K. D. Cancer Statistics , 2019. doi:10.3322/caac.21551.

16. Chaudhary, B. & Elkord, E. Regulatory T Cells in the Tumor Microenvironment and Cancer Progression : Role and Therapeutic Targeting. **3**, 1–25.

17. Dowling, M. R. *et al.* Regulatory T Cells Suppress Effector T Cell Proliferation by Limiting Division Destiny. **9**, 1–10 (2018).

18. Ward-hartstonge, K. A. & Kemp, R. A. Regulatory T-cell heterogeneity and the cancer immune response. *Nat. Publ. Gr.* (2017) doi:10.1038/cti.2017.43.

19. Takeuchi, Y. & Nishikawa, H. Roles of regulatory T cells in cancer immunity. **28**, 401–409 (2016).

20. Gebhardt, C. *et al.* Myeloid Cells and Related Chronic In fl ammatory Factors as Novel Predictive Markers in Melanoma Treatment with Ipilimumab. 5453–5459 doi:10.1158/1078-0432.CCR-15-0676.

21. Meyer, C. *et al.* Frequencies of circulating MDSC correlate with clinical outcome of melanoma patients treated with ipilimumab. 247–257 (2014) doi:10.1007/s00262-013-1508-5.

22. Holmgaard, R. B., Zamarin, D. & Lesokhin, A. EBioMedicine Targeting myeloid-derived suppressor cells with colony stimulating factor-1 receptor blockade can reverse immune resistance to immunotherapy in indoleamine 2 , 3-dioxygenase-expressing tumors. *EBIOM* **6**, 50–58 (2016).

23. Kubala, M. H., Placencio, V. R. & DeClerck, Y. A. Abstract 3061: Tumor-derived PAI-1 promotes macrophage M2 polarization by stimulating an autocrine IL-6 /STAT3 pathway. *Cancer Res.* **77**, 3061 (2017).

24. Meri, R. R. & Puolakkainen, P. A. ScienceDirect Tumor-associated macrophages (TAMs) as biomarkers for gastric cancer : A review. **4**, 156–163 (2018).

25. Mantovani, A. *et al.* Infiltration of tumours by macrophages and dendritic cells: tumour-associated macrophages as a paradigm for polarized M2 mononuclear

phagocytes. *Novartis Found. Symp.* **256**, 137-138,259-269 (2004).

26. Hartley, G. P., Chow, L., Ammons, D. T., Wheat, W. H. & Dow, S. W. Programmed Cell Death Ligand 1 (PD-L1) Signaling Regulates Macrophage Proliferation and Activation. **1**, 1260–1273 (2018).

27. Gabrilovich, D. I. & Nagaraj, S. Myeloid-derived suppressor cells as regulators of the immune system. **9**, (2009).

28. Lindau, D., Gielen, P., Kroesen, M. & Wessel-, P. The immunosuppressive tumour network : myeloid-derived suppressor cells , regulatory T cells and natural killer T cells. doi:10.1111/imm.12036.

29. Khaled, Y. S., Ammori, B. J. & Elkord, E. Myeloid-derived suppressor cells in cancer : recent progress and prospects. 493–502 (2013) doi:10.1038/icb.2013.29.

30. Engelman, J. A. & Settleman, J. Acquired resistance to tyrosine kinase inhibitors during cancer therapy. **2**,.

31. Therapeutics, M. The KRAS-G12C inhibitor : activity and resistance. **2021**, (2021).

32. Oatman, N. *et al.* Mechanisms of stearoyl CoA desaturase inhibitor sensitivity and acquired resistance in cancer. 1–20 (2021).

33. Bedard, P. L., Hansen, A. R., Ratain, M. J. & Siu, L. L. Tumour heterogeneity in the clinic. **24**, (2013).

34. Xue, G. *et al.* blockade via the concurrent depletion of tumour. **5**, (2021).

35. Schoenfeld, A. J. & Hellmann, M. D. Acquired Resistance to Immune Checkpoint Inhibitors. *Cancer Cell* **37**, 443–455 (2020).

36. Draghi, A., Chamberlain, C. A., Furness, A., Donia, M. & Donia, M. Acquired resistance to cancer immunotherapy. 31–40 (2019).

37. Petitprez, F., Meylan, M., de Reyniès, A., Sautès-Fridman, C. & Fridman, W. H. The Tumor Microenvironment in the Response to Immune Checkpoint Blockade Therapies. *Front. Immunol.* **11**, 1–11 (2020).

38. Tang, H., Li, H. & Sun, Z. Targeting myeloid-derived suppressor cells for cancer therapy. *Cancer Biol. Med.* **18**, 992–1009 (2021).

39. Lin, Y., Xu, J. & Lan, H. Tumor-associated macrophages in tumor metastasis : biological roles and clinical therapeutic applications. **3**, 1–16 (2019).

40. Mathew, J. M. *et al.* A Phase I Clinical Trial with Ex Vivo Expanded Recipient Regulatory T cells in Living Donor Kidney Transplants. 1–12 (2018) doi:10.1038/s41598-018-25574-7.

41. Tobin, R. *et al.* Targeting MDSCs using ATRA : a phase I / II clinical trial combining pembrolizumab and all-trans retinoic acid for metastatic melanoma.

42. Liu, Y. & Cao, X. Immunosuppressive cells in tumor immune escape and metastasis. *J. Mol. Med.* 509–522 (2016) doi:10.1007/s00109-015-1376-x.

43. Gyori, D. *et al.* Compensation between CSF1R + macrophages and Foxp3 + Treg cells drives resistance to tumor immunotherapy. 1–12.

44. Tanaka, A. & Sakaguchi, S. Regulatory T cells in cancer immunotherapy. *Nat. Publ. Gr.* 109–118 (2017) doi:10.1038/cr.2016.151.

45. Colombo, M. P. & Piconese, S. Regulatory T-cell inhibition versus depletion : the right choice in cancer immunotherapy.

46. Saleh, R. & Elkord, E. Seminars in Cancer Biology Acquired resistance to cancer immunotherapy : Role of tumor-mediated immunosuppression. *Semin. Cancer Biol.* **65**, 13–27 (2020).

47. Buckner, J. H. Mechanisms of impaired regulation T cells in human autoimmune diseases. *Nat. Publ. Gr.* **10**, 849–859 (2010).

48. Xue, G., Jin, G., Fang, J. & Lu, Y. IL-4 together with IL-1β induces antitumor Th9 cell differentiation in the absence of TGF-β signaling. *Nat. Commun.* **10**, 1–10 (2019).

49. Mao, C., Li, F., Zhao, Y., Debinski, W. & Ming, X. T h e r a n o s t i c s P-glycoprotein-targeted photodynamic therapy boosts cancer nanomedicine by priming tumor microenvironment. **8**, (2018).

50. Sato, K. *et al.* Spatially selective depletion of tumor-associated regulatory T cells with near-infrared photoimmunotherapy. **8**, (2016).

51. Mitsunaga, M., Ogawa, M., Kosaka, N., Rosenblum, L. T. & Choyke, P. L. Cancer cell – selective in vivo near infrared photoimmunotherapy targeting specific membrane molecules. *Nat. Med.* **17**, 1685–1692 (2011).

52. Sato, K., Nagaya, T., Mitsunaga, M., Choyke, P. L. & Kobayashi, H. Near infrared photoimmunotherapy for lung metastases. *Cancer Lett.* **365**, 112–121 (2015).

53. Mellman, I., Coukos, G. & Dranoff, G. Cancer immunotherapy comes of age. *Nature* (2011) doi:10.1038/nature10673.

54. Wang, Y. *et al.* Photodynamic therapy of pancreatic cancer: Where have we come from and where are we going? *Photodiagnosis Photodyn. Ther.* **31**, 101876 (2020).

55. Tuit, S. *et al.* Transcriptional Signature Derived from Murine Tumor-Associated Macrophages Correlates with Poor Outcome in Breast Cancer Patients Article Transcriptional Signature Derived from Murine Tumor-Associated Macrophages Correlates with Poor Outcome in Breast Can. *CellReports* **29**, 1221-1235.e5 (2019).

56. Elpek, K. G. *et al.* The Tumor Microenvironment Shapes Lineage , Transcriptional , and Functional Diversity of In fi ltrating Myeloid Cells. 655–667 doi:10.1158/2326-6066.CIR-13-0209.

57. Goswami, S. *et al.* Immune profiling of human tumors identifies CD73 as a combinatorial target in glioblastoma. *Nat. Med.* **26**, (2020).

58. Azambuja, J. H. *et al.* Blockade of CD73 delays glioblastoma growth by modulating the immune environment. *Cancer Immunol. Immunother.* **69**, 1801–1812 (2020).

59. Buisseret, L. *et al.* Clinical significance of CD73 in triple-negative breast cancer: Multiplex analysis of a phase III clinical trial. *Ann. Oncol.* **29**, 1056–1062 (2018).

60. Neel, D. S. & Bivona, T. G. Resistance is futile : overcoming resistance to targeted therapies in lung adenocarcinoma. *npj Precis. Oncol.* 1–5 (2017) doi:10.1038/s41698-017-0007-0.

61. Agarwal, R. & Kaye, S. B. OVARIAN CANCER : STRATEGIES FOR OVERCOMING RESISTANCE TO CHEMOTHERAPY. **3**, 502–516 (2003).

62. Li, K. *et al.* Myeloid-derived suppressor cells as immunosuppressive regulators and therapeutic targets in cancer. *Signal Transduct. Target. Ther.* (2021) doi:10.1038/s41392-021-00670-9.

63. Vijayan, D., Young, A., Teng, M. W. L. & Smyth, M. J. Targeting immunosuppressive adenosine in cancer. *Nat. Publ. Gr.* **17**, 709–724 (2017).

64. Mixed Reviews for A2AR Inhibitor in NSCLC. *Cancer Discov.* **9**, OF2–OF2 (2019).

65. Stagg, J. *et al.* Anti-CD73 antibody therapy inhibits breast tumor growth and metastasis. *Proc. Natl. Acad. Sci. U. S. A.* **107**, 1547–1552 (2010).

66. Mathias, U. *et al.* Tissue-based map of the human proteome. *Science (80-.).* **347**, 1260419 (2015).

67. Monteiro, I. *et al.* CD73 expression and clinical significance in human metastatic melanoma. *Oncotarget* **9**, 26659–26669 (2018).

68. Sciarra, A. *et al.* CD73 expression in normal and pathological human hepatobiliopancreatic tissues. *Cancer Immunol. Immunother.* **68**, 467–478 (2019).

Ziyu (Blake) Wang

2907 Prescott St., Houston, TX, 77025 | (614)441-1016 | ziywang@wakehealth.edu | blakewang110@gmail.com

Professional Summary

To continue my research on utilizing CAR T cells and other immunomodulating agents to treat cancers, I want to pursue a graduate academic position that can help me augment my levels of research skills and knowledge in the cancer therapy field and further expand my views to other correlated areas.

Education

Ohio State University, College of Arts and Science
August 2016 – May 2020
Bachelor of Science, Pre-Health Professional
Major: Biology

Wake Forest University, Graduate School of Arts and Science
August 2020 – May 2022
Master of Science, Biomedical Science
Awarded BMSC MS Scholarship: 2020-2021 ($18,660), 2021-2022 ($23,550).

Skills & Abilities

Lab Skills

- Proficient in using microscope, spectrometer, micropipette in biology-related labs
- Basic data collection, t-Test, one-way ANOVA, and two-way ANOVA
- Human and mice tumor and immune cell culturing
- Cell viability testing
- General PCR and Real time qPCR
- Western blot
- ELISA
- Isolation of human and mice PBMCs, T cells, and NKT cells.
- Isolation of donor tumor-infiltrating lymphocytes
- Mice colon organoid construction
- Flow cytometry and cell sorting
- Traditional lentiviral and retroviral transfection
- Electroporation transfection

- Mice intravenous injection, intraperitoneal injection, subcutaneous injection, intratibial injection, and caudal arterial injection.

Language

- Proficient in English communication
- Proficient in Chinese communication

Computer

- Proficient in utilizing Word, PowerPoint, Excel, JMP software, Adobe Premiere, FACSDiva, Flowjo, Prism Graphpad, IVIS Living Imaging Software, and Photo Shop.

Research Experiences

Undergraduate Student Volunteer Research Assistant

September 2019 – July 2020

Ohio State University, James Comprehensive Cancer Center

Lab PI and mentor: Zihai Li, li.10950@osu.edu, (614)366-0172

Lab co-mentor: Xingjun Wu, wu.4727@osu.edu, (614)688-3716

- Worked on checking the stability and persistence of Grp94/gp96 chaperone protein expressions on surface and intracellular environment by generating Grp94 knockdown HuH-7.5 cells.
- Worked on the project of inhibiting Grp94 in 293FT cells to check and determine its effects on neutralizing SARS-CoV-2 infection.
- Worked on the construction of CAR T cell regarding generating 4D3 CAR T with isolated $CD3^+$ cells and *in vivo* cytotoxicity assay with Grp94 knockdown liver tumor HuH-7.5.
- ULAR Rodent Training regarding mice handling and blood collections for general animal experiments.

Graduate Student Research Assistant

August 2020 – Present

Wake Forest Baptist Health, School of Medicine

Lab PI and mentor: Yong Lu, yolu@wakehealth.edu, ylu2@houstonmethodist.org

- Performed the experiments about overcoming the acquired resistance to PD-1 blockade, from breast cancer and pancreatic cancer, by simultaneously depleting tumor and immunosuppressive cells via the combinational therapy of anti-CD73 with near-infrared-irradiation and PD-1 ICB.
    - Conducted *in vivo* experiments and helped construct the figures.
- Worked on the screening of FDA-approved drug library in eradicating ovarian tumor and Burkitts Lymphoma cells with CAR T cells.
    - Conducted both *in vitro* and *in vivo* tests with mice models.
- Worked on the construction of multiple myeloma MM.1S and ARP-1 cell lines with CRISPR/Cas9 human-genome knockout genes to test the resistance to chemotherapy drug.

- Worked on the projects about overcoming primary and acquired resistance by inducing tumor cell death via oncolytic virus and CAR T cells.

Projects and Publications

Projects

- Combining nanoparticle-cGAMP with HER2-CAR T to suppress Lewis lung carcinoma metastasis in mice models.
- Utilizing CRISPR/Cas9 to generate human genome-wide knockout multiple myeloma cell lines to screen out the genes that are associated with the resistance of the tumor to some clinical immune-modulating drugs.
- Isolating iNKT from human PBMC and expanding them to build CD19-CAR T to treat Burkitts Lymphoma.

Publications

Xue G, W Ziyu, Zheng N, Jing Fang, Mao C, Li X, Jin G, Ming X, and Yong Lu. Elimination of acquired resistance to PD-1 blockade via the concurrent depletion of tumor cells and immunosuppressive cells. Nature Biomedical Engineering. 2021.

Zheng N, F Jing, Xue G, Wang Z, Li X, Zhou M, Jin G, Rahman M, Grant McFadden, and Yong Lu. Induction of tumor cell death by oncolytic virus and CAR-T cells overcome primary and acquired resistance. Cancer Cell. 2022. (Submitted for Initial Review)

Additional Experience

Part-time Teaching Assistant for *TOEFL and SAT*

June 2016 – July 2018

Imagination Education, Henan, China

Employer: Jun Song

- Assisting the instructors for TOEFL and SAT courses by explaining in-class questions to students, taking notes of their in-class performance, and sending the records to their guardians.